Nano Energy 78 (2020) 105312

Contents lists available at ScienceDirect

Nano Energy

journal homepage: http://www.elsevier.com/locate/nanoen

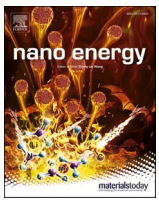

# Flexible GaN microwire-based piezotronic sensory memory device

Qilin Hua [a,b], Junlu Sun [a], Haitao Liu [a], Xiao Cui [a,b], Keyu Ji [a,c], Wenbin Guo [a,b], Caofeng Pan [a,b,c,d,***], Weiguo Hu [a,b,c,*], Zhong Lin Wang [a,b,e,**]

[a] CAS Center for Excellence in Nanoscience, Beijing Key Laboratory of Micro-nano Energy and Sensor, Beijing Institute of Nanoenergy and Nanosystems, Chinese Academy of Sciences, Beijing, 100083, China
[b] School of Nanoscience and Technology, University of Chinese Academy of Sciences, Beijing, 100049, PR China
[c] Center on Nanoenergy Research, School of Physical Science and Technology, Guangxi University, Nanning, Guangxi, 530004, PR China
[d] College of Physics and Optoelectronic Engineering, Shenzhen University, Shenzhen, 518060, China
[e] School of Materials Science and Engineering, Georgia Institute of Technology, Atlanta, GA, 30332-0245, USA

ARTICLE INFO

*Keywords:*
GaN
Micro/nanowire
Piezotronics
Sensory memory
Artificial intelligence

ABSTRACT

Skin-inspired electronic devices that can store and retain impressions of sensory information after the removal of external stimuli are showing great significance for artificial sensory systems. Here, a single GaN microwire-based piezotronic sensory memory device (SMD) is presented to sense and memorize the impressions of tactile information. The SMD is capable to be programmed into a high resistance state by inputting external strain, and reversibly erased back to the low resistance state with an electrical voltage. Due to the piezotronic effect, the piezo-potential induced by compressive strain would cause the dissolution/redistribution of conductive channels of nitrogen vacancies in the bamboo-shaped GaN microwire. Furthermore, the SMD array demonstrates a distinct spatial mapping of external strain sensing and retaining with the operations of strain program and electrical erase. The single micro/nanowire-based sensory memory device will have great applications in the field of tactile sensation, touchable haptic technologies, and bio-realistic artificial intelligence systems.

## 1. Introduction

Sensory memory can automatically store and retain impressions of sensory information that is perceived by receptors in the human body after the removal of external stimuli [1]. It helps to keep an accurate and very brief buffer for the stimuli of the five senses (*i.e.*, sight, hearing, smell, taste, and touch) into the brain, which is very essential for us interacting with the surroundings. Among the five senses, the sense of touch is of great importance to allow us to possess tactile perception and feedback in virtual and real environments [2], due to the sensation functionalities of human skin. Many kinds of electronic devices have been developed to emulate the sense of touch, which is also called electronic skin (or e-skin) [3–5], based on the mechanisms of capacitance [6,7], piezoresistivity [8,9], piezoelectricity [10,11], and triboelectricity [12,13]. Commonly, those reported devices only provide the tactile sensation, however, not capable to retain the memory/impression of tactile information. Learning from the biological sensory memory, it is very necessary to develop e-skin with the capabilities of tactile perception and storage. Zhu et al. reported a haptic memory device composed of a resistive pressure sensor (micro-structured PDMS film embedded with silver nanowires) and a resistive switching memory cell (metal-insulator-metal architecture with $SiO_2$) to provide the retaining of pressure information [14]. Similarly, Chen et al. also used the combined device with a resistive switching memory cell (metal-insulator-metal architecture with $Al_2O_3$) and a resistive image sensor ($In_2O_3$ based UV sensor) to construct an artificial visual memory system [15]. However, those devices are very complicated in integration, and inevitably limit the large-scale array applications. Indeed, a simple device that can sense and memorize the tactile information remains a great challenge for artificial sensory systems.

* Corresponding author. CAS Center for Excellence in Nanoscience, Beijing Key Laboratory of Micro-nano Energy and Sensor, Beijing Institute of Nanoenergy and Nanosystems, Chinese Academy of Sciences, Beijing, 100083, China.
** Corresponding author. CAS Center for Excellence in Nanoscience, Beijing Key Laboratory of Micro-nano Energy and Sensor, Beijing Institute of Nanoenergy and Nanosystems, Chinese Academy of Sciences, Beijing, 100083, China.
*** Corresponding author. CAS Center for Excellence in Nanoscience, Beijing Key Laboratory of Micro-nano Energy and Sensor, Beijing Institute of Nanoenergy and Nanosystems, Chinese Academy of Sciences, Beijing, 100083, China.
*E-mail addresses:* cfpan@binn.cas.cn (C. Pan), huweiguo@binn.cas.cn (W. Hu), zhong.wang@mse.gatech.edu (Z.L. Wang).

https://doi.org/10.1016/j.nanoen.2020.105312
Received 12 June 2020; Received in revised form 9 August 2020; Accepted 21 August 2020
Available online 27 August 2020

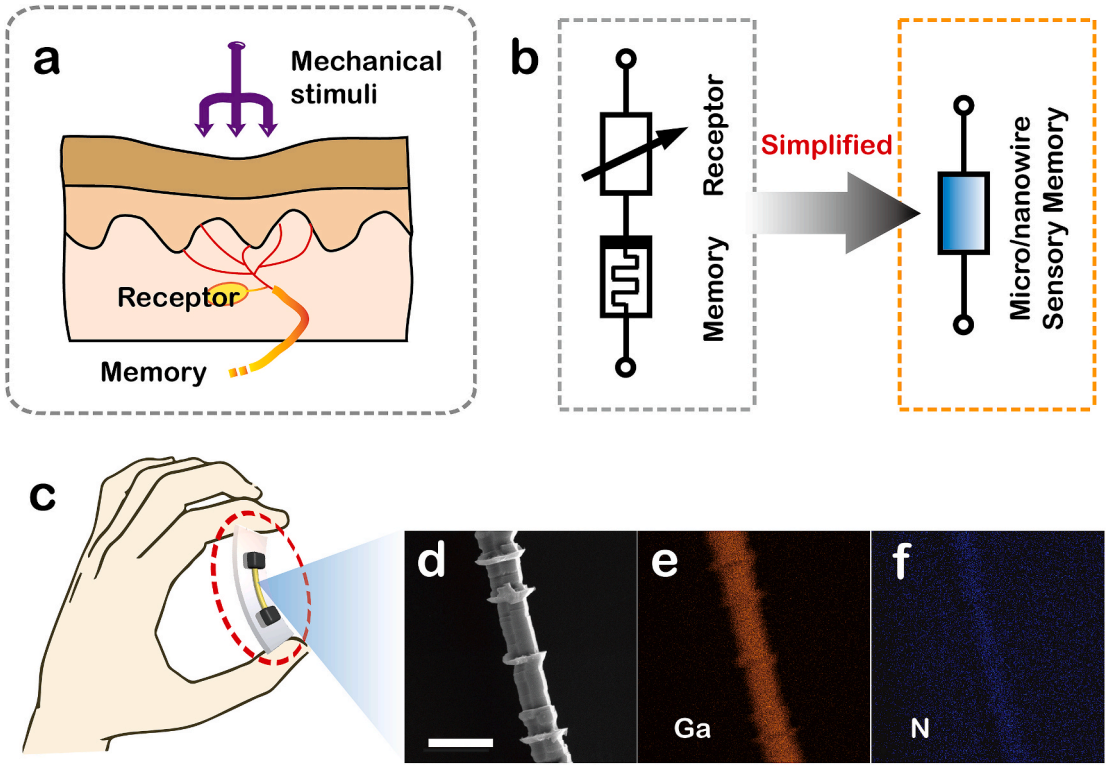


**Fig. 1.** GaN micro/nanowire-based piezotronic sensory memory device (SMD). (a) Schematic illustration of the sensory memory system in human skin, which is composed of receptors and memory units. Upon an external force applied on the skin, the mechanical stimulus is perceived by the sensory receptors with retaining the sensory impression, and processed by the central nervous system. (b) The equivalent circuit of the SMD. A receptor and a memory unit are connected in series to form the sensory memory in human skin, which can be simplified into an individual device by using a single micro/nanowire. (c) Schematic illustration for GaN microwire-based SMD pinched by a hand. (d) Scanning electron microscopy (SEM) image of a single GaN microwire, which shows the bamboo-shaped structure. Scale bar: 2 μm. (e,f) Energy-dispersive X-ray spectroscopy (EDS) mapping of Ga and N, respectively.

By coupling two effects of piezoelectricity and semiconductor, the piezotronic micro/nanowire semiconductors, *e.g.*, ZnO [10,11,16], and GaN [17–19], are demonstrated to have the capability of pressure or strain sensing with high sensitivity, high resolution, and large-scale fabrication/integration [10,11,16,20,21]. According to the piezotronic effect, the introduced pressure or strain allows the semiconductor to produce piezoelectric polarization charges at the interface, which will tune the interface barrier or control charge carrier transport characteristics [20,21]. In addition, many types of piezotronic devices are also reported, including sensors [22,23], LEDs [11,24,25], solar cells [26,27], memristors [19,28], HEMTs [29,30], topological-insulator-based [31,32], and synapses [33]. And thus with expectations, the piezotronic device will have potential applications for tactile information sensation and storage.

Here, we present a GaN microwire-based piezotronic sensory memory device (SMD) that can memorize the input strain in resistance state after the strain ceased, and also be reversibly erased with electrical voltage bias. The impressions of tactile information are easily retained in the single micro/nanowire-based device configuration, leading to the reduction of the complexity of the artificial sensory memory systems. Upon the piezotronic effect, the piezo-potential generated by the applied compressive strain is used to induce the formation of nitrogen vacancies that could act as electron traps to form/dissolve electron transport channels at the knots of the bamboo-shaped GaN microwire. The multiple resistance states are tuned in response to different compressive strain. Furthermore, the sensory memory mapping illustrations of the 3 × 3 SMD array are demonstrated for the external strain sensing and retaining with the operations of strain program and electrical erase.

## 2. Results and discussion

Fig. 1 illustrates the novel concept of GaN microwire-based SMD. The biological sensory memory system in human skin is typically composed of receptors and memory units, as schematically shown in Fig. 1a. Upon an external force applied on the skin, the mechanical stimulation is perceived by the sensory receptors and retained the tactile impression by the memory unit after the initial stimulation has ceased, and finally processed by the central nervous system. As inspired by the biological model, an electronic device based on GaN microwire is introduced to demonstrate the functionalities of the sensory memory system. The equivalent circuits of the biological model and the SMD are shown in Fig. 1b. In contrast to the combination of a receptor and a memory unit, the artificial sensory memory can be simplified into an individual device by using a single piezotronic micro/nanowire (*e.g.*, GaN microwire).

The schematic illustrates that the SMD can be pinched by a hand, indicating the strain program operation, as illustrated in Fig. 1c. The GaN micro/nanowires were synthesized by chemical vapor deposition (CVD) with liquid Ga source precursor and 50 sccm $NH_3$ flow at a high temperature of 950 °C for 8 h. The structural morphology of GaN is observed by a scanning electron microscopy (SEM) (Fig. 1d), and the corresponding elemental profiles of Ga and N are captured by the energy-dispersive X-ray spectroscopy (EDS) mapping (Fig. 1e and f). Thus it can be seen that the GaN microwire has a bamboo-shaped structure. From Fig. 1e and f, the N distribution seems a little different from the Ga distribution, especially in the bamboo-shaped knot regions (although the contrast not so clear). As liquid Ga as the source, the GaN micro/nanowire would grow along the *c*-axis with the rapid nitridation of Ga by dissociated ammonia at the high temperature [19]. During the process of growth, the vapor pressure of Ga could alter and induce some Ga-rich regions, leading to further radial formation of the

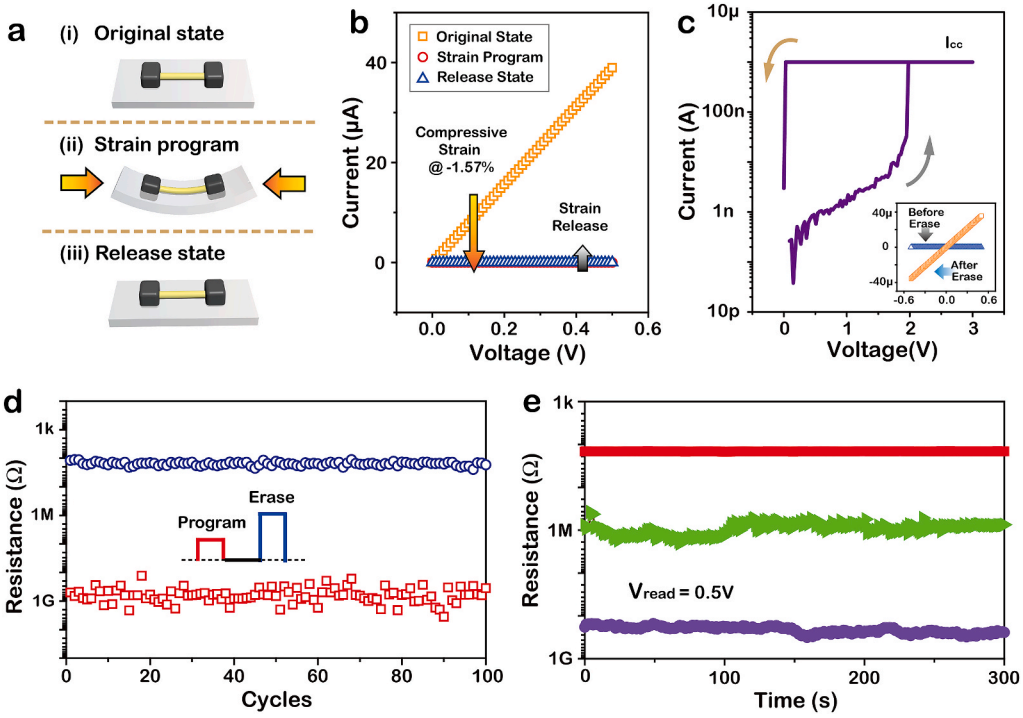


**Fig. 2.** Electrical performances of the SMD. (a) Schematic illustration for the strain program operation of the SMD. (b) I–V characteristics of the SMD in strain program, including original state, loading a compressive strain of −0.57%, and strain release state. (c) I–V characteristics of the SMD in electrical erase at a compliance current ($I_{cc}$) of 1 μA. The inset is the I–V characteristics at the voltage sweep from −0.5 V to 0.5V for the cases before and after electrical erase. (d) Endurance performance of the SMD for 100 cycles with strain program of −1.57% and electrical erase of 3 V. (e) Retention performance of the SMD with multilevel states (*i.e.*, three stain states) at a read voltage ($V_{read}$) of 0.5 V.

bamboo-shaped knots (*i.e.*, nitrogen deficiency regions). In addition, the fabrication process of the SMD is introduced as follows: the single GaN micro/nanowire is transferred onto a polystyrene (PS) substrate, and source/drain electrodes are prepared at the two ends of the GaN microwire with silver paste connection into Cu wires.

The as-fabricated SMD has good flexibility, and can be well applied to strain program and electrical erase operations. Fig. 2a illustrates the strain program (or write) operation of the SMD. The operation contains three steps: original state, strain program, and release state. Upon bending, the SMD is programmed (or written) by loading a compressive strain. And then, the SMD is capable of retaining the resistance state after releasing the strain, which corresponds to the basis for the biological sensory memory. The DC I–V characteristics of the SMD are measured by a Keysight B1500A semiconductor device parameter analyzer. Fig. 2b shows the typical I–V characteristics of the SMD with a strain program operation. By loading a compressive strain of −1.57%, the resistance of the SMD exhibits a pronounced transition from a low resistance state (LRS) of 10-kΩ-scale to a high resistance state (HRS) of 100-MΩ-scale. After releasing the compressive strain, the I–V curves show no obvious changes when compared to the one under strain, indicating the good performance for memorizing the impressions of tactile information in the SMD. Furthermore, the typical I–V characteristics of the SMD with an electrical erase operation is shown in Fig. 2c. The SMD is firstly programmed into a HRS of 100-MΩ-scale (*e.g.*, 877.2

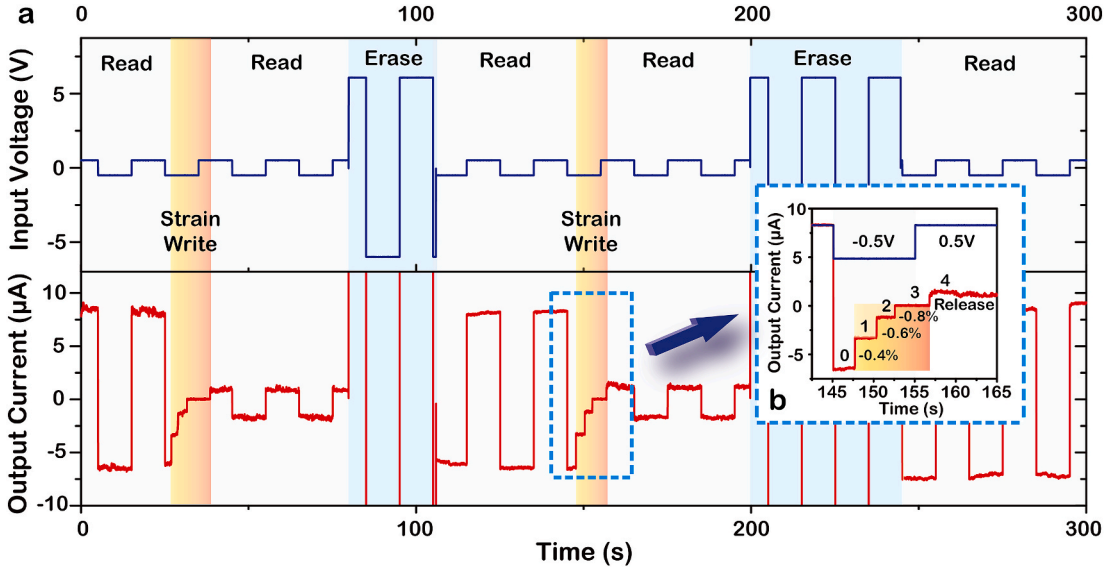


**Fig. 3.** Write/erase operations of the SMD. (a) Output currents response to 0.1 Hz square-wave input voltage biases during the serial operations including resistance read, strain write, and electrical erase. Read voltage bias is 0.5 V, and electrical erase voltage bias is 6 V. (b) The enlarged view at the cyan dashed triangle in (a), showing the detailed changes of the output current with applying three different compressive strain (−0.4%, −0.6%, and −0.8%).

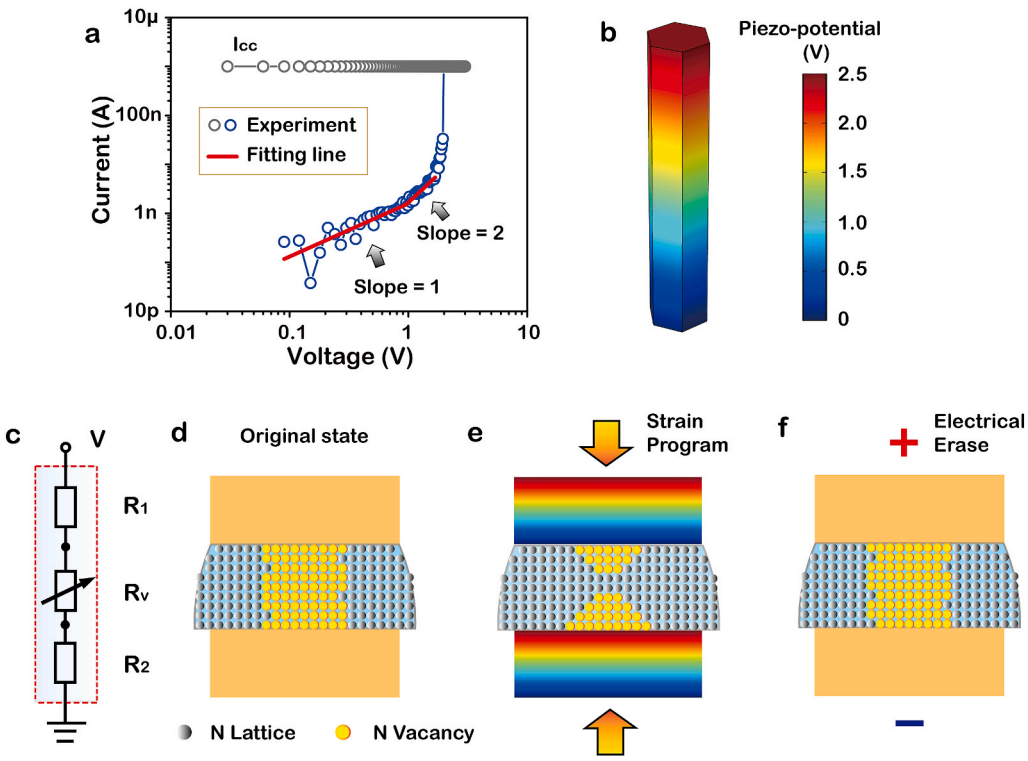


**Fig. 4.** Working mechanism of the SMD. (a) Double-logarithm I–V characteristics of the SMD, indicating the space charge limited conduction (SCLC) mechanism. (b) Finite element analysis for the piezo-potential distribution of the hexagonal GaN microwire (length = 5 μm, diameter = 1 μm) under a compressive strain of −0.5% (COMOSOL Multiphysics). (c) The simplified equivalent circuits of the GaN microwire. The resistors ($R_1$ and $R_2$) indicate the smooth crystal regions of the GaN microwire, while the variable resistor ($R_V$) corresponds to the knot region. Upon loading a voltage on the device, the current can flow from the drain to the source, and certainly pass across the knot regions. (d–f) Schematic illustrations for the working mechanism of the SMD, including (d) original state, (e) strain program, and (f) electrical erase. Nitrogen vacancies ($V_N$) could act as electron traps to form/dissolve electron transport channels at the knots of the bamboo-shaped GaN microwire.

MΩ) after inputting and releasing the compressive strain. And then, the HRS can be erased back into the LRS of 10-kΩ-scale (*e.g.*, 14.0 kΩ), when applying the voltage sweeps from 0 to 3 V. It is remarkable that the SMD can be programmed into the HRS under the compressive strain and also erased back to the LRS again in a highly reversible manner, indicating the good performance of artificial sensory memory. Specifically, the good endurance performance of the SMD is well demonstrated for 100 cycles under the repeatable operations including strain program of −1.57% and electrical erase voltage of 3 V, as shown in Fig. 2d. In addition, compared with the very brief retention (<1 s) of the biological sensory memory, the SMD exhibits a better retention performance over 300 s with multilevel states (*e.g.*, three strain states at 0%, −1.03%, and −1.34%), as shown in Fig. 2e.

To illustrate the continuous read/write/erase operations in temporal scale, a computer-controlled measurement system composed of a function generator (DS345, Stanford Research Systems), a low-noise current preamplifier (SR570, Stanford Research Systems), and a GPIB controller (GPIB-USB-HS, NI 488.2) is used to conduct electrical measurement of output current with square-wave input bias. And a typical SMD in the same batch is chosen as the device under test. Fig. 3a clearly shows the sequential read/write/erase operations of the SMD. The output currents response to 0.1 Hz square-wave input voltage biases during the serial operations including resistance read, strain write, and electrical erase. In the beginning, the resistance of the SMD is at a LRS of 60 kΩ when applying a read voltage bias of 0.5 V. And then, the resistance transits into a HRS of 600 kΩ after a load of a compressive strain of −0.8% at steps. Consequently, the resistance can transit back to the LRS of 60 kΩ by applying a large voltage bias of 6 V. Fig. 3b shows the detailed changes of the output current by applying three different compressive strain (*i.e.*, −0.4%, −0.6%, and −0.8%) and then releasing the strain. The resistance of the SMD shows a step-like transition into HRS with the increase of the compressive strain, and the HRS remains to be holding even after releasing the strain.

Based on the double-logarithm I–V characteristics of the SMD in Fig. 4a, the trap-controlled space-charge-limited-conduction (SCLC) theory [34,35] could be used to elucidate the working mechanism of the SMD. Commonly, the trap-controlled SCLC consists of three regions, including Ohmic region ($I \sim V$), Child's square law (trap-unfilled SCLC) region ($I \sim V^2$), and the current increase in the high field (trap-filled SCLC) region [35]. In the HRS (blue curve in Fig. 4a), the three regions with evident slope difference well agree to the trap-controlled SCLC theory. In the LRS (orange curve in Fig. 2c), Ohmic conduction would be induced by the formation of nitrogen vacancies ($V_N$) due to the applying of a large voltage bias. Actually, the knot region of the bamboo-shaped GaN microwire filled with a large amount of $V_N$ (*i.e.*, nitrogen deficiency) is considered as a variable barrier [19], and the $V_N$ acting as trap states contributes to the transport of electrons [36,37]. Fig. 4b illustrates the calculated piezo-potential distribution of the hexagonal GaN microwire (length = 5 μm, diameter = 1 μm) under a compressive strain of −0.5%. The induced piezo-potential might be as high as 2.5 V. As it is previously reported, the introducing electric field could induce the formation of vacancy [38]. The movement of $V_N$ under electric field is probably responsible for the switching phenomenon [39]. And consequently, the piezo-potential would effectively induce the formation (or dissolution) of conductive channel of $V_N$ in the GaN microwire by the applied compressive strain, which would be different from the common piezotronic modulation at the interfacial Schottky barrier or p-n junction [20,21].

It is remarkable that the working mechanism of the SMD is attributed to $V_N$ acting as electron traps for the formation/rupture of conductive channel with electrons trapping and detrapping procedures. Fig. 4c shows the simplified equivalent circuits of the GaN microwire in the SMD to indicate the corresponding resistors in the schematic illustrations of Fig. 4d–f. Among them, the knot region can be considered as a variable resistor ($R_V$), which would principally affect the transport of electrons. Furthermore, the dynamic evolutions of conductive channel of $V_N$ are schematically shown in Fig. 4d–f. Initially, a large amount of trap states (*e.g.*, $V_N$) would form a large conductive channel in the GaN microwire (probably at the knots), thus leading to the Ohmic conduction behavior (Fig. 4d). Upon a load of a compressive strain, the induced piezo-potential would reduce the thickness (or rupture) of the conductive channel, resulting in the resistance transition into HRS (Fig. 4e).

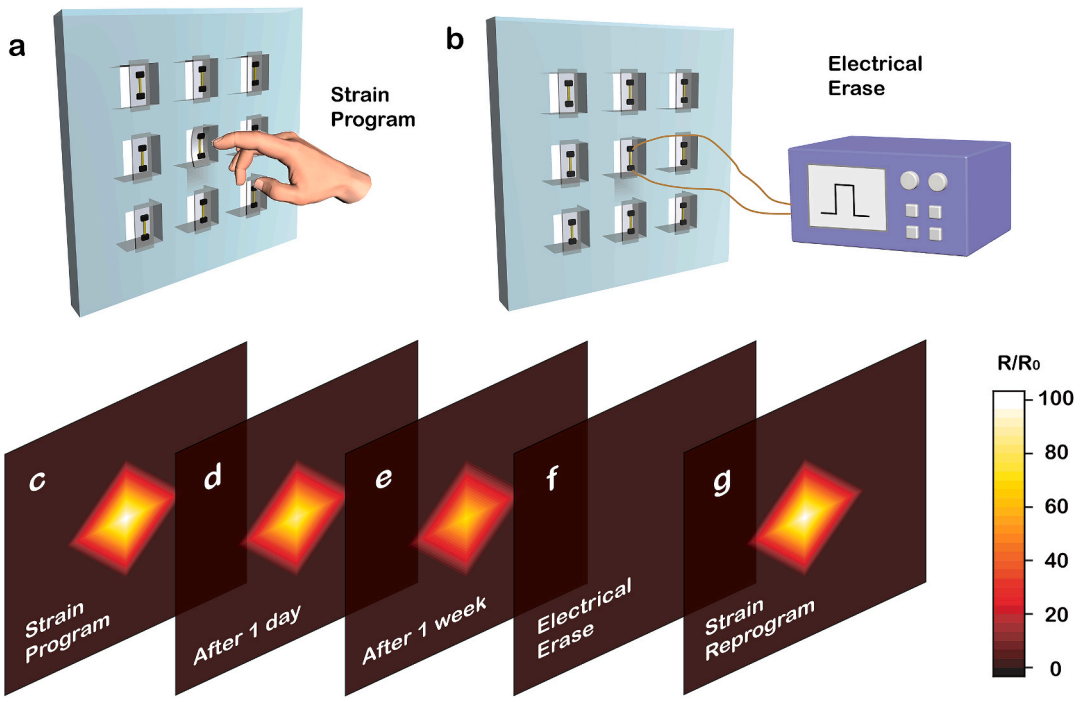


**Fig. 5.** Sensory memory mapping demonstration of the SMD array. (a,b) Schematic illustrations for the operations of the 3 × 3 SMD array in (a) strain program and (b) electrical erase, respectively. (c–g) Mapping illustrations of the SMD array for the external strain sensing and retaining at the state of (c) strain program, (d) after 1 day, (e) after 1 week, (f) electrical erase, and (g) strain reprogram.

After releasing the compressive strain, the SMD can also retain the resistance at HRS. Furthermore, by applying a critical voltage bias, the conductive channel would grow into the large one again, leading to the resistance transition back to LRS (Fig. 4f). In short, the conductive channel composed of $V_N$ will become thinner (or rupture) under the operation of strain program, while it will grow thicker under the operation of electrical erase. And hence, the SMD can well perform in a good reproducible manner under the operations of strain program and electrical erase, also showing the promising potential for human-machine interfaces and artificial sensory systems applications.

In order to illustrate the touchable haptic memory panel, a SMD array with 3 × 3 pixels is fabricated to demonstrate the capability of mapping and memorizing strain distribution after the removal of the strain. The schematic illustrations for the operations of strain program and electrical erase are shown in Fig. 5a and b, respectively. In the 3 × 3 SMD array panel, a finger makes a strain on a pixel of the array to do the write operation, leading to the distinct spatial mapping of external strain; and the electrical erase operation is applied by giving a voltage bias on the device. As shown in Fig. 5c, the SMD array can clearly record the applied strain and its corresponding position/distribution, *i.e.*, a strain of −1.2% loaded at the center of pixels. Moreover, the SMD array is also devoted to memorizing the strain mapping even after one day or one week with small variation or decay, as illustrated in Fig. 5d and e, respectively. In addition, the strain mapping can further be erased by voltage sweep (Fig. 5f), and reprogrammed with strain loaded on the SMD (Fig. 5g). As described above, the reconfigurable SMD array achieves the capability of strain information mapping and retaining as the recess of the strain or voltage in multi-cycle operations.

## 3. Conclusions

In summary, the flexible GaN microwire-based piezotronic sensory memory device is demonstrated to be capable of strain sensing and memorizing, which contributes to the reduction of the complexity of the artificial sensory memory systems. The SMD can be programmed into HRS by applying external strain in multi-states, and also be reversibly erased with electrical voltage bias. The working mechanism of the SMD is attributed to nitrogen vacancies acting as electron traps to form/dissolve electron transport channels at the knots of the bamboo-shaped GaN microwire. Due to the piezotronic effect, the compressive strain is used to induce the formation of nitrogen vacancies in the GaN microwire, thus leading to the thickness reduction (or rupture) of the conductive channel (*i.e.*, resistance transition into HRS). Moreover, the sensory memory mapping illustrations of the 3 × 3 SMD array are demonstrated for the external strain sensing and retaining with the operations of strain program and electrical erase. The SMD enables the retaining of touch and haptic experiences in a single micro/nanowire-based sensory memory system, and will contribute to the development of tactile sensation and touchable haptic technologies, promoting advances in bio-realistic artificial intelligence systems.

## CRediT authorship contribution statement

**Qilin Hua:** Conceptualization, Methodology, Writing - review & editing, Visualization, Funding acquisition. **Junlu Sun:** Validation, Software. **Haitao Liu:** Methodology, Validation, Investigation. **Xiao Cui:** Investigation. **Keyu Ji:** Investigation. **Wenbin Guo:** Investigation. **Caofeng Pan:** Supervision, Resources, Funding acquisition. **Weiguo Hu:** Writing - review & editing, Supervision, Project administration, Funding acquisition. **Zhong Lin Wang:** Writing - review & editing, Supervision, Funding acquisition.

## Declaration of competing interest

The authors declare that they have no known competing financial interests or personal relationships that could have appeared to influence the work reported in this paper.

## Acknowledgements

Q.H., J.S., and H.L. contributed equally to this work. The authors thank for the support from the National Key Research and Development

Program of China (2016YFA0202703), the National Natural Science Foundation of China (61904012, 61704008, 51622205, 61675027, 61505010 and 51502018), the Beijing City Committee of science and technology (Z171100002017019 and Z181100004418004), the Natural Science Foundation of Beijing Municipality (4204114, 4181004, 4182080, 4184110, 2184131 and Z180011), and the University of Chinese Academy of Sciences.

## References

[1] E. vKöster, J. Mojet, in: J. Hort, S.E. Kemp, T. Hollowood (Eds.), Time-Dependent Measures of Perception in Sensory Evaluation, John Wiley & Sons Ltd, West Sussex, UK, 2017. Ch. 5.
[2] G. Robles-De-La-Torre, IEEE MultiMedia 13 (2006) 24.
[3] S. Wang, J. Xu, W. Wang, G.N. Wang, R. Rastak, F. Molina-Lopez, J.W. Chung, S. Niu, V.R. Feig, J. Lopez, T. Lei, S.K. Kwon, Y. Kim, A.M. Foudeh, A. Ehrlich, A. Gasperini, Y. Yun, B. Murmann, J.B. Tok, Z. Bao, Nature 555 (2018) 83.
[4] A. Chortos, J. Liu, Z. Bao, Nat. Mater. 15 (2016) 937.
[5] Q. Hua, J. Sun, H. Liu, R. Bao, R. Yu, J. Zhai, C. Pan, Z.L. Wang, Nat. Commun. 9 (2018) 244.
[6] C. Pang, J.H. Koo, A. Nguyen, J.M. Caves, M.G. Kim, A. Chortos, K. Kim, P.J. Wang, J.B. Tok, Z. Bao, Adv. Mater. 27 (2015) 634.
[7] X. Zhao, Q. Hua, R. Yu, Y. Zhang, C. Pan, Adv. Electron. Mater. 1 (2015) 1500142.
[8] L. Pan, A. Chortos, G. Yu, Y. Wang, S. Isaacson, R. Allen, Y. Shi, R. Dauskardt, Z. Bao, Nat. Commun. 5 (2014) 3002.
[9] Y. Kim, A. Chortos, W. Xu, Y. Liu, J.Y. Oh, D. Son, J. Kang, A.M. Foudeh, C. Zhu, Y. Lee, S. Niu, J. Liu, R. Pfattner, Z. Bao, T.-W. Lee, Science 360 (2018) 998.
[10] W. Wu, X. Wen, Z.L. Wang, Science 340 (2013) 952.
[11] C. Pan, L. Dong, G. Zhu, S. Niu, R. Yu, Q. Yang, Y. Liu, Z.L. Wang, Nat. Photon. 7 (2013) 752.
[12] X. Pu, M. Liu, X. Chen, J. Sun, C. Du, Y. Zhang, J. Zhai, W. Hu, Z.L. Wang, Sci. Adv. 3 (2017), e1700015.
[13] L. Lin, Y. Xie, S. Wang, W. Wu, S. Niu, X. Wen, Z.L. Wang, ACS Nano 7 (2013) 8266.
[14] B. Zhu, H. Wang, Y. Liu, D. Qi, Z. Liu, H. Wang, J. Yu, M. Sherburne, Z. Wang, X. Chen, Adv. Mater. 28 (2015) 1559.
[15] S. Chen, Z. Lou, D. Chen, G. Shen, Adv. Mater. 30 (2018) 1705400.
[16] Z.L. Wang, J. Song, Science 312 (2006) 242.
[17] R. Yu, L. Dong, C. Pan, S. Niu, H. Liu, W. Liu, S. Chua, D. Chi, Z.L. Wang, Adv. Mater. 24 (2012) 3532.
[18] Z. Zhao, X. Pu, C. Han, C. Du, L. Li, C. Jiang, W. Hu, Z.L. Wang, ACS Nano 9 (2015) 8578.
[19] H. Liu, Q. Hua, R. Yu, Y. Yang, T. Zhang, Y. Zhang, C. Pan, Adv. Funct. Mater. 26 (2016) 5307.
[20] W. Wu, Z.L. Wang, Nat. Rev. Mater. 1 (2016) 16031.
[21] C. Pan, J. Zhai, Z.L. Wang, Chem. Rev. 119 (2019) 9303.
[22] X. Wang, J. Zhou, J. Song, J. Liu, N. Xu, Z.L. Wang, Nano Lett. 6 (2006) 2768.
[23] X. Han, W. Du, R. Yu, C. Pan, Z.L. Wang, Adv. Mater. 27 (2015) 7963.
[24] Q. Yang, W. Wang, S. Xu, Z.L. Wang, Nano Lett. 11 (2011) 4012.
[25] Y. Hu, Y. Zhang, L. Lin, Y. Ding, G. Zhu, Z.L. Wang, Nano Lett. 12 (2012) 3851.
[26] G. Hu, W. Guo, R. Yu, X. Yang, R. Zhou, C. Pan, Z.L. Wang, Nano Energy 23 (2016) 27.
[27] J. Sun, Q. Hua, R. Zhou, D. Li, W. Guo, X. Li, G. Hu, C. Shan, Q. Meng, L. Dong, C. Pan, Z.L. Wang, ACS Nano 13 (2019) 4507.
[28] W. Wu, Z.L. Wang, Nano Lett. 11 (2011) 2779.
[29] S. Zhang, B. Ma, X. Zhou, Q. Hua, J. Gong, T. Liu, X. Cui, J. Zhu, W. Guo, L. Jing, W. Hu, Z.L. Wang, Nat. Commun. 11 (2020) 326.
[30] J. Zhu, X. Zhou, L. Jing, Q. Hua, W. Hu, Z.L. Wang, ACS Nano 13 (2019) 13161.
[31] M. Dan, G. Hu, L. Li, Y. Zhang, Nano Energy 50 (2018) 544.
[32] G. Hu, L. Li, Y. Zhang, Nano Energy 59 (2019) 667.
[33] Q. Hua, X. Cui, H. Liu, C. Pan, W. Hu, Z.L. Wang, Nano Lett. 20 (2020) 3761.
[34] D. Ielmini, Y. Zhang, J. Appl. Phys. 102 (2007), 054517.
[35] E. Lim, R. Ismail, Electronics 4 (2015) 586.
[36] Y. Chen, H. Song, H. Jiang, Z. Li, Z. Zhang, X. Sun, D. Li, G. Miao, Appl. Phys. Lett. 105 (2014) 193502.
[37] K. Fu, H. Fu, X. Huang, T. Yang, H. Chen, I. Baranowski, J. Montes, C. Yang, J. Zhou, Y. Zhao, IEEE Electron. Device Lett. 40 (2019) 375.
[38] J. Jeong, N. Aetukuri, T. Graf, T.D. Schladt, M.G. Samant, S.S.P. Parkin, Science 339 (2013) 1402.
[39] B.J. Choi, A.C. Torrezan, J.P. Strachan, P.G. Kotula, A.J. Lohn, M.J. Marinella, Z. Li, R.S. Williams, J.J. Yang, Adv. Funct. Mater. 26 (2016) 5290.

**Dr. Qilin Hua** received his Ph.D. degree in microelectronics from University of Chinese Academy of Sciences in 2016. He then joined Tsinghua University, China. He is currently an associate professor at Beijing Institute of Nanoenergy and Nanosystems, Chinese Academy of Science. His research interests include flexible/stretchable electronics, low-dimensional materials, GaN-based devices, memristors, and neuromorphic systems.

**Junlu Sun** received his Master's degree in Materials Science & Engineering from Zhengzhou University in 2014. He is currently a Ph. D. Candidate majored in Optics at Zhengzhou University. He has joined in the group of Professor Caofeng Pan at Beijing Institute of Nanoenergy and Nanosystems, CAS as a visiting student since 2015. His research focuses on flexible thin film perovskite solar cells and piezotronic/piezophototronic effects of nano-devices.

**Xiao Cui** received his B.S. degree from Xidian University in 2016. He is pursuing his M.S. degree in condensed matter physics at University of Chinese Academy of Sciences since 2017. His research interests focus on GaN-based power devices and the piezotronic effect.

**Prof. Caofeng Pan** received his B.S. degree (2005) and Ph.D. degree (2010) in Materials Science and Engineering from the Tsinghua University, China. He then joined the group of Prof. Zhong Lin Wang at the Georgia Institute of Technology as a postdoctoral fellow from 2010 to 2013. He is currently a professor and a group leader at the Beijing Institute of Nanoenergy and Nanosystems, Chinese Academy of Sciences. His research interests mainly focus on the fields of piezotronics/piezophototronics for fabricating new electronic and optoelectronic devices, nanopower source, hybrid nanogenerators, and self-powered nanosystems. Details can be found at http://www.piezotronics.cn/.

**Prof. Weiguo Hu** is a principal investigator at the Beijing Institute of Nanoenergy and Nanosystems, Chinese Academy of Science (CAS), China. He received his PhD degree from the Institute of Semiconductors, CAS, in 2007. His research focuses on gallium nitride-based piezotronic/piezo-phototronic devices and wearable self-powered nanosystems. He has authored more than 70 peer-reviewed journal articles in these fields.

**Prof. Zhong Lin (Z L) Wang** received his Ph.D. from Arizona State University in physics. He now is the Hightower Chair in Materials Science and Engineering, Regents' Professor, Engineering Distinguished Professor and Director, Center for Nanostructure Characterization, at Georgia Tech. Dr. Wang has made original and innovative contributions to the synthesis, discovery, characterization and understanding of fundamental physical properties of oxide nanobelts and nanowires, as well as applications of nanowires in energy sciences, electronics, optoelectronics and biological science. His discovery and breakthroughs in developing nanogenerators established the principle and technological road map for harvesting mechanical energy from environment and biological systems for powering personal electronics. His research on self-powered nanosystems has inspired the worldwide effort in academia and industry for studying energy for micro-nano-systems, which is now a distinct disciplinary in energy research and future sensor networks. He coined and pioneered the field of piezotronics and piezo-phototronics by introducing piezoelectric potential gated charge transport process in fabricating new electronic and optoelectronic devices.